NASA TECHNICAL MEMORANDUM

UB
NASA TM X-1210

UB
NASA TM X-1210

CLASSIFICATION CHANGED TO UNCLASSIFIED
AUTHORITY: NASA DIS Memo
DATED 5-8-75
L.E. Mann
(Signature)
10-27-77
(Date)

A SUMMARY OF X-15 HEAT-TRANSFER AND SKIN-FRICTION MEASUREMENTS

by Richard D. Banner and Albert E. Kuhl

Flight Research Center
Edwards, Calif.

NATIONAL AERONAUTICS AND SPACE ADMINISTRATION • WASHINGTON, D. C. • FEBRUARY 1966

NASA TM X-1210

A SUMMARY OF X-15 HEAT-TRANSFER AND SKIN-FRICTION MEASUREMENTS

By Richard D. Banner and Albert E. Kuhl

Flight Research Center
Edwards, Calif.

NATIONAL AERONAUTICS AND SPACE ADMINISTRATION

A SUMMARY OF X-15 HEAT-TRANSFER AND SKIN-FRICTION MEASUREMENTS* **

By Richard D. Banner and Albert E. Kuhl
Flight Research Center

SUMMARY

Measured local Mach numbers and heat transfer obtained on the lower surface of the X-15 wing and bottom centerline of the fuselage at angles of attack up to 18° and on the vertical fin with both a sharp and a blunt leading edge are summarized and compared with calculations using Eckert's reference-temperature method. Direct measurements of skin friction on the surface of the sharp-leading-edge vertical fin are also presented. It is shown that both the heat-transfer and skin-friction data can be predicted by neglecting the effect of wall temperature in the calculation of the reference temperature by Eckert's method.

Uncertainties in level and trend of Reynolds analogy factor with Mach number are discussed, and a planned flight investigation is described.

INTRODUCTION

The preliminary data (ref. 1) reported at the 1961 Conference on the Progress of the X-15 Project indicated the turbulent heat transfer measured on the X-15 to be lower than accepted methods would predict. Eckert's reference-temperature method (ref. 2), or Sommer and Short's T-prime method (ref. 3), and Van Driest's theory (ref. 4) are interpreted as having been acceptable, in that each conservatively predicts an increase in heat transfer with increased heat rate (lower wall-to-adiabatic-wall temperature ratios). The early X-15 results (ref. 1) were of considerable interest, since the X-15 data were obtained at conditions where the little data that existed showed contradicting trends (that is, at low wall-to-adiabatic-wall temperature ratios). From the preliminary analysis (ref. 1), it appeared that the effect of wall temperature on turbulent heat transfer was less than the accepted methods would predict and could possibly be neglected.

---

*Title, Unclassified.

**This paper was included in a classified report entitled "Fourth Conference on Progress of the X-15 Research Airplane Program," Flight Research Center, Oct. 7, 1965. NASA SP-90, 1965.

At that time, only flight data acquired during the X-15 performance-expansion program were available. Since then, a series of flights has been made specifically to obtain heat-transfer and local-flow data. Attention has been directed to three principal areas on the X-15: the wing midsemispan, the fuselage bottom centerline, and the vertical tail. (See fig. 1.) In these areas the geometry of the flow is known best and is the least difficult to measure. Impact-pressure rakes were installed at the locations shown, and local-flow conditions were measured.

SYMBOLS

C_f	local skin-friction coefficient, $\frac{\tau}{q_l}$
C_{f_i}	incompressible value of the local skin-friction coefficient
c_p	specific heat of air at constant pressure, $\frac{\text{Btu}}{\text{lb-}^\circ\text{F}}$
h	heat-transfer coefficient, $\frac{\text{Btu}}{\text{ft}^2\text{-}^\circ\text{F-sec}}$
M	Mach number
q	dynamic pressure, pounds per square foot
R_x	Reynolds number, $\frac{\rho_l V_l x}{\mu_l}$
St	Stanton number, $\frac{h}{\rho_l V_l c_{p_l}}$
St_i	incompressible value of the Stanton number
T_W	wall (or surface) temperature, °R
T_R	boundary-layer recovery (or adiabatic wall) temperature, °R
$\frac{u_L}{u_\infty}$	ratio of the laminar sublayer to boundary-layer-edge velocities for a flat plate
V	velocity, feet per second
x	length, feet
α	angle of attack, degrees

μ coefficient of viscosity, pounds per foot-second

ρ density, pounds per cubic foot

τ surface shear, pounds per square foot

Subscripts:

l local

∞ free stream

DISCUSSION

Flow Conditions

In order to correlate the heat-transfer data, the boundary-layer-edge flow conditions must be known. In the preliminary analysis, the local-flow conditions were approximated by use of attached-shock methods. In a subsequent analysis of heat-transfer data obtained during the first flight to Mach 6, the local properties were based on calculated detached-shock flow conditions (ref. 5). The rake measurements permitted a check of the analytical methods.

In a study made at the NASA Flight Research Center by Palitz, calculated and measured local Mach numbers on the wing, fuselage, and vertical fin are compared. Examples of these comparisons are shown in figure 2. The characteristic shear layers produced by the detached shocks from the blunt leading edges are to be noted. An example of the differences in flow conditions behind a blunt and a sharp leading edge is shown in the vertical-fin data. The fin was modified from the normally blunt 0.5-inch-radius leading edge to a sharp 0.015-inch-radius leading edge. Data are included for both configurations. The reduction in local Mach number due to increased bluntness can be seen. In general, good agreement between measured and calculated local Mach numbers has been obtained over a wide range of conditions. Note that the data near the surface of the wing, the fuselage (at zero angle of attack), and the blunt vertical tail fall below the calculated values. This is to be expected, since the inviscid shear-layer calculations do not account for the viscous boundary layer. The Moeckel-Love calculation procedure is described in reference 5. The boundary-layer heights, shown by the arrows, have been estimated by the methods given in references 6 and 7. Note that the measured local Mach numbers drop below the calculated inviscid values at about the estimated boundary-layer heights.

For the fuselage nose location at an angle of attack of 10°, the boundary-layer thickness is estimated to be less than the height of the innermost probe. In cases of this type, the calculated surface Mach numbers have been used to approximate the boundary-layer-edge Mach numbers. For the sharp-leading-edge fin, the calculations show that the shear layer is confined to a narrow region near the surface. In this instance, the boundary-layer edge is in essentially uniform flow. By using the methods just described, the Mach numbers at the boundary-layer edge have been obtained with reasonably good accuracy at all locations.

Heat Transfer

Other boundary-layer-edge conditions (density, velocity, and static temperature) were derived from isentropic-flow relationships. These, in turn, were used with the measured heat-transfer coefficients to obtain dimensionless Stanton numbers for correlation of the data at all locations. At some locations it was necessary to include internal conduction effects when reducing the measured skin-temperature data to heat-transfer coefficients. The largest effect of conduction losses occurred in the data from the wing and the vertical fin, where corrections up to 18 percent were required.

The wing and fuselage data at low angles of attack from the first flight to Mach 6 (ref. 5) and the blunt- and the sharp-leading-edge fin data (ref. 8), shown in terms of the ratio of the compressible Stanton number to the incompressible value, are plotted against local Mach number in figure 3. For comparison purposes, the variation in the Stanton number ratio given by Eckert's reference-temperature method (ref. 2) is shown for two wall-temperature values that bracket the range of the test data. Although it might be expected that the data would fall throughout this bounded region if the effect of wall temperature were as predicted by Eckert's method, most of the data fall near and slightly below the lower boundary given by assuming the wall temperature to be equal to the boundary-layer recovery temperature. Some data are as much as 35 percent less than values predicted by Eckert's reference-temperature method.

A similar trend has also been noted in data recently obtained at the Flight Research Center by Quinn on the X-15 wing and fuselage at angles of attack up to 18° (fig. 4). The wall-to-recovery temperature ratio for these data varied from 0.35 to 0.70. For comparison, the Stanton number ratio that would be calculated by Eckert's method at a wall temperature equal to one-half the recovery temperature is shown. Again, the data are scattered near the level predicted by assuming the wall temperature to be equal to the recovery temperature.

Eckert's method has been used for comparison with the X-15 data because of its general acceptance and use. Also, this method best illustrates the large effect that wall temperature was previously thought to have on heat transfer. Eckert's method agrees closely with the T-prime method (ref. 3), which has been shown to agree particularly well with measured skin friction (ref. 9) at adiabatic-wall conditions $(T_W = T_R)$. It is believed that the X-15 results have contributed to a renewed interest in more accurately defining the trend in turbulent heat transfer and skin friction at low wall-to-recovery temperatures.

The effect of low wall temperature has been reexamined by Spalding and Chi (ref. 10), Danberg (ref. 11), Bartz (ref. 12), and more recently by Bertram and Neal (ref. 13). These studies have also indicated that the effect of wall temperature is less than previously thought, but sufficient data to define the exact trend and level are not available.

Most of the methods for calculating turbulent heat transfer have been based on analyses of turbulent skin friction and the use of Reynolds analogy factor. Several methods for predicting turbulent skin friction are compared in figure 5. The incompressible skin-friction values given by the methods noted have been normalized with respect to the values given by Blasius--the method used to compute the incompressible Stanton numbers for the X-15 data--and are plotted against Reynolds number.

These methods are described in reference 14. It is noted in the figure that over the X-15 Reynolds number range there would be only about a 10-percent difference in the calculated skin-friction coefficient, regardless of the method used. The simpler Blasius equation, which has been used for X-15 correlation, gives a good average skin-friction level over the X-15 range.

After the skin-friction equation to be used is selected, a Reynolds analogy factor is needed in order to compute the Stanton number. The available data are compared in figure 6 with values given by Dorrance (ref. 15) and Rubesin (ref. 16). Most of the data at low wall-to-recovery temperature ratios have been obtained indirectly from boundary-layer temperature and velocity surveys (refs. 17 to 19). Recent data obtained by Peterson at the NASA Langley Research Center are also shown. These data show a wide variation, about 40 percent. Direct measurements (refs. 13 and 20) have given values between 1.15 and 1.35, which are nearer the predictions and fall about the level found by Colburn (ref. 21) in low-speed pipe-flow experiments. Bertram and Neal (ref. 13) applied the incompressible Von Kármán equation to compressible flow and found good agreement with Neal's direct measurements. For the X-15 data correlation, Colburn's modified Reynolds analogy factor was used. Clearly, additional data are needed.

Skin Friction

An experiment is planned in which skin friction and heat transfer will be measured simultaneously on the sharp-leading-edge fin of the X-15 airplane in order to obtain Reynolds analogy-factor data. Some preliminary skin-friction measurements have been made at the Flight Research Center by Garringer at speeds up to Mach 5 by using a direct-reading skin-friction balance installed in the fin surface. Data from two flights are shown in figure 7 as the ratio of the measured skin-friction coefficient to the incompressible skin-friction coefficient plotted against local Mach number. As for the heat-transfer data, the local conditions were derived from measured surface static and impact pressures and isentropic relationships.

The balance was mounted in a manner that produced a longitudinal surface-temperature gradient ahead of the sensing element. The exact effect of this gradient on the measurement is not known. Considering only the surface-temperature levels, values of the wall-to-recovery temperature ratio near the element varied with local Mach number, as shown in the plot at the upper right of the figure. Values between 0.3 and 1.3 were experienced during the flight. The data, however, do not show the effect of this parameter that would be predicted by Eckert's reference-temperature method; the values obtained during both increasing and decreasing speeds are more nearly approximated by assuming the wall temperature to be equal to the recovery temperature.

CONCLUDING REMARKS

From this preliminary analysis, it appears that both the turbulent heat transfer and skin friction measured on the X-15 may be correlated in the same manner, that is, by neglecting the effect of wall temperature in the calculation of the reference temperature. This result suggests that the Reynolds analogy factor is essentially constant for the X-15 heating conditions.

More conclusive results are anticipated from future tests on the X-15 during which skin-friction, heat-transfer, and boundary-layer-noise measurements will be made simultaneously. In addition to obtaining data under the normal X-15 surface-heating conditions, it appears that data could be obtained at "very cold wall" conditions. The means of obtaining a "very cold wall" would be similar to the technique used in Project Fire--the instrumented surface would be suddenly exposed to high heating by releasing an insulating cover. Initial wall-to-recovery temperature ratios would be near $T_W/T_R = 0.2$. The high heating rates would improve the accuracy in deriving heat-transfer coefficients from the measured skin temperatures and, with simultaneous measurement of the surface shear, Reynolds analogy factor would be obtained.

Flight Research Center
National Aeronautics and Space Administration
Edwards, Calif., October 7, 1965.

REFERENCES

1. Banner, Richard D.; Kuhl, Albert E.; and Quinn, Robert D.: Preliminary Results of Aerodynamic Heating Studies on the X-15 Airplane. NASA TM X-638, 1962.

2. Eckert, Ernst R. G.: Survey on Heat Transfer at High Speeds. WADC Tech. Rep. 54-70 (Contract No. AF 33(616)-2214, RDO No. 474-143), Wright Air Dev. Center, U.S. Air Force, Apr. 1954.

3. Sommer, Simon C.; and Short, Barbara J.: Free-Flight Measurements of Turbulent-Boundary-Layer Skin Friction in the Presence of Severe Aerodynamic Heating at Mach Numbers From 2.8 to 7.0. NACA TN 3391, 1955.

4. Van Driest, E. R.: The Problem of Aerodynamic Heating. Aero. Eng. Rev., vol. 15, no. 10, Oct. 1956, pp. 26-41.

5. Quinn, Robert D.; and Kuhl, Albert E.: Comparison of Flight-Measured and Calculated Turbulent Heat Transfer on the X-15 Airplane at Mach Numbers From 2.5 to 6.0 at Low Angles of Attack. NASA TM X-939, 1964.

6. Reshotko, Eli; and Tucker, Maurice: Approximate Calculation of the Compressible Turbulent Boundary Layer With Heat Transfer and Arbitrary Pressure Gradient. NACA TN 4154, 1957.

7. Persh, Jerome; and Lee, Roland: Tabulation of Compressible Turbulent Boundary Layer Parameters. NAVORD Rep. 4282, U.S. Naval Ordnance Lab. (White Oak, Md.), May 1, 1956.

8. Banas, Ronald P.: Comparison of Measured and Calculated Turbulent Heat Transfer in a Uniform and Nonuniform Flow Field on the X-15 Upper Vertical Fin at Mach Numbers of 4.2 and 5.3. NASA TM X-1136, 1965.

9. Matting, Fred W.; Chapman, Dean R.; Nyholm, Jack R.; and Thomas, Andrew G.: Turbulent Skin Friction at High Mach Numbers and Reynolds Numbers in Air and Helium. NASA TR R-82, 1961.

10. Spalding, D. B.; and Chi, S. W.: The Drag of a Compressible Turbulent Boundary Layer on a Smooth Flat Plate With and Without Heat Transfer. J. Fluid Mech., vol. 18, part I, Jan. 1964, pp. 117-143.

11. Danberg, James E.: Characteristics of the Turbulent Boundary Layer With Heat and Mass Transfer at M=6.7. NOLTR 64-99, U.S. Naval Ordnance Lab. (White Oak, Md.), Oct. 19, 1964.

12. Bartz, D. R.: Turbulent Boundary-Layer Heat Transfer From Rapidly Accelerating Flow of Rocket Combustion Gases and of Heated Air. Vol. 2 of Advances in Heat Transfer, James P. Hartnett and Thomas F. Irvine, Jr., eds., Academic Press, 1965.

13. Bertram, Mitchell H.; and Neal, Luther, Jr.: Recent Erperiments in Hypersonic Turbulent Boundary Layers. Presented at the AGARD Specialists Meeting on Recent Developments in Boundary-Layer Research (Naples, Italy), May 10-14, 1965.

14. Schlichting, Hermann: Boundary Layer Theory. Fourth ed., McGraw-Hill Book Co., Inc., 1960.

15. Dorrance, William H.: Viscous Hypersonic Flow. Theory of Reacting and Hypersonic Boundary Layers. McGraw-Hill Book Co., Inc., 1962, p. 189.

16. Rubesin, Morris W.: A Modified Reynolds Analogy for the Compressible Turbulent Boundary Layer on a Flat Plate. NACA TN 2917, 1953.

17. Winkler, Eva M.; and Cha, Moon H.: Investigation of Flat Plate Hypersonic Turbulent Boundary Layers With Heat Transfer at a Mach Number of 5.3. NAVORD Rep. 6631, U.S. Naval Ordnance Lab. (White Oak, Md.), Sept. 15, 1959.

18. Hill, F. K.: Turbulent Boundary Layer Measurements at Mach Numbers From 8 to 10. The Physics of Fluids, vol. 2, no. 6, Nov.-Dec., 1959.

19. Lobb, R. K.; Winkler, Eva M.; and Persh, Jerome: NOL Hypersonic Tunnel No. 4 Results VII: Experimental Investigation of Turbulent Boundary Layers in Hypersonic Flow. NAVORD Rep. 3880, U.S. Naval Ordnance Lab. (White Oak, Md.), Mar. 1, 1955.

20. Rochelle, William C.: Prandtl Number Distribution in a Turbulent Boundary Layer With Heat Transfer at Supersonic Speeds. DRL-508, Defense Research Lab., Univ. of Texas. Oct. 1963.

21. Colburn, A. P.: A Method of Correlating Forced Convection Heat-Transfer Data and a Comparison With Fluid Friction. Trans. Amer. Inst. Chem. Eng., vol. 29, 1933, pp. 174-210.

X-15 HEAT-TRANSFER TEST AREAS

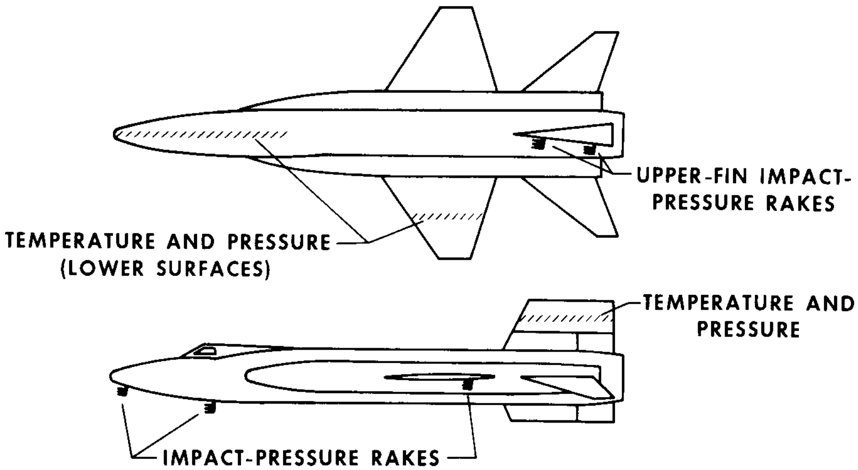

Figure 1

SHEAR-LAYER PROFILES

$M_\infty = 4$

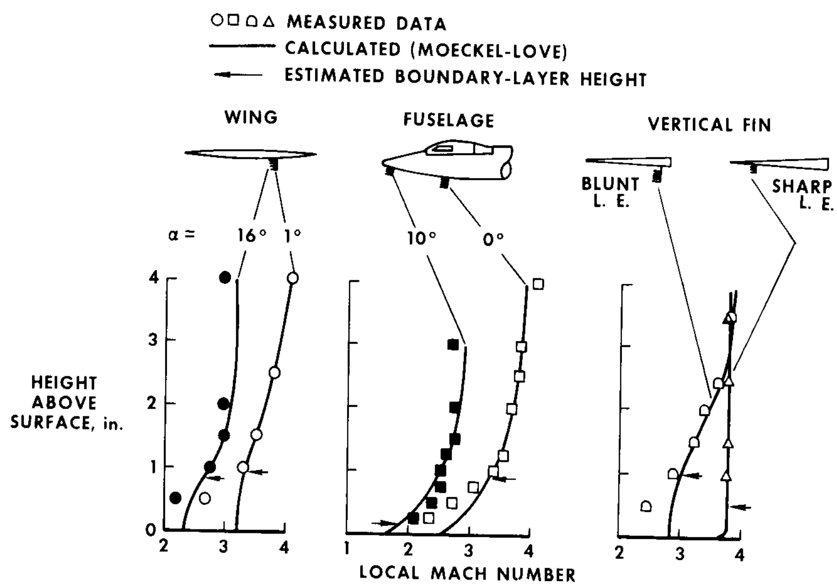

Figure 2

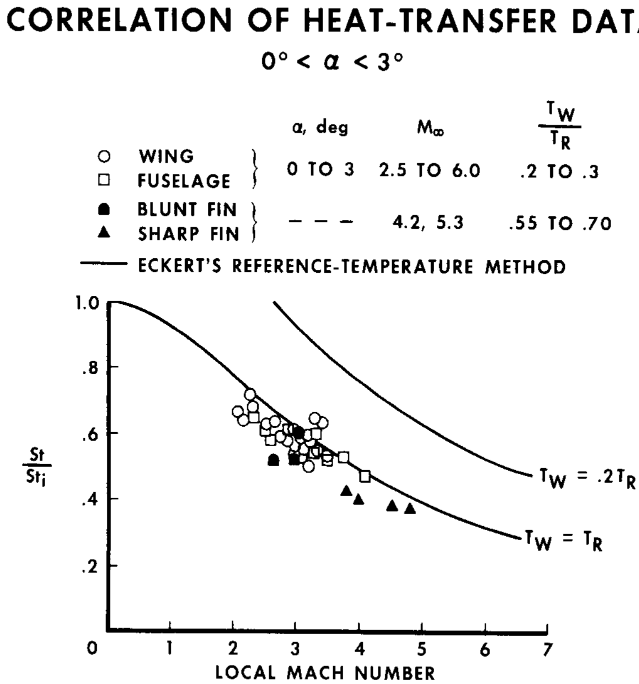

Figure 3

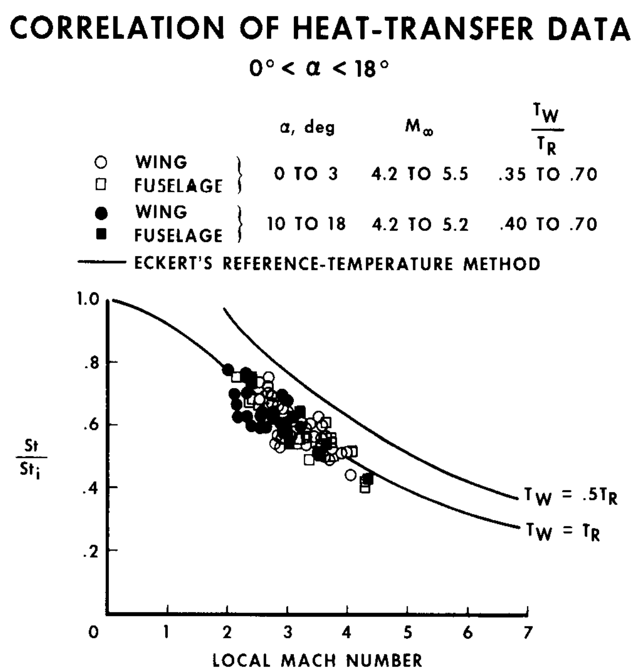

Figure 4

COMPARISON OF TURBULENT-RESISTANCE FORMULAS

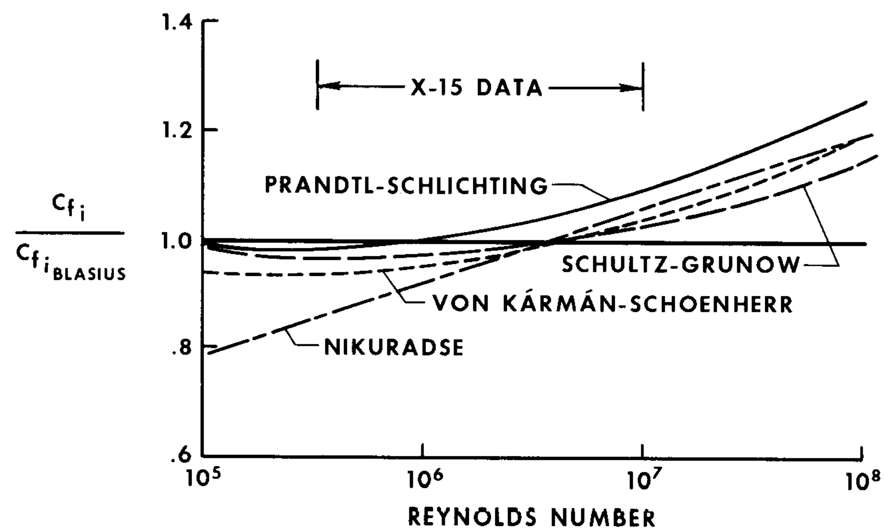

Figure 5

VARIATION OF REYNOLDS ANALOGY FACTOR WITH MACH NUMBER

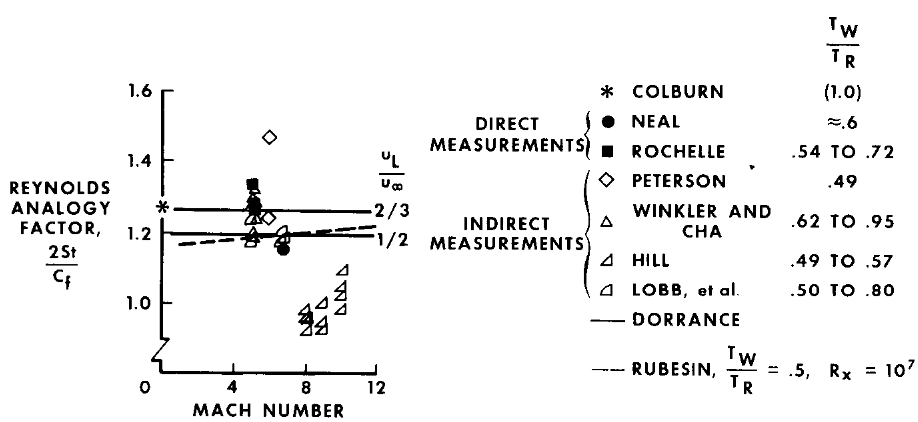

Figure 6

PRELIMINARY X-15 SKIN-FRICTION RESULTS
DIRECT-READING BALANCE

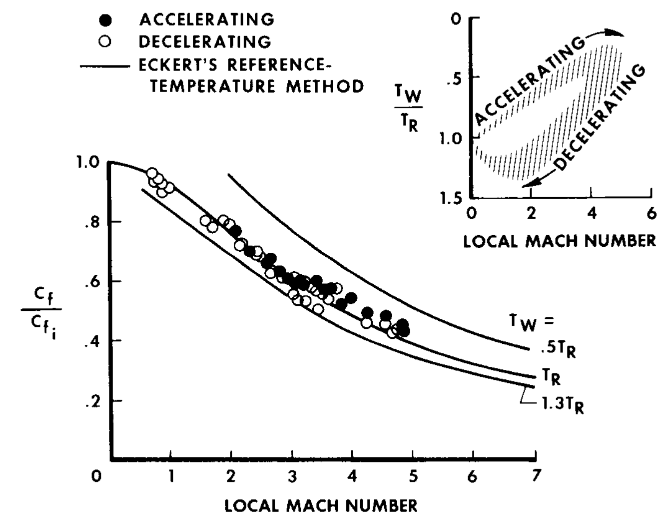

Figure 7

NASA-Langley, 1966 H-416